Natural Hazards
https://doi.org/10.1007/s11069-022-05380-1

ORIGINAL PAPER

Monitoring and projection of climate change impact on 24-h probable maximum precipitation in the Southeast of Caspian Sea

Zahra Afzali-Gorouh[1] · Alireza Faridhosseini[1] · Bahram Bakhtiari[2] · Abolfazl Mosaedi[1] · Nasrin Salehnia[3,4]

Received: 11 October 2021 / Accepted: 19 April 2022

Abstract
Due to the impacts of climate change on probable maximum precipitation (PMP) and its importance in designing hydraulic structures, PMP estimation is crucial. In this study, the effect of climate change on 24-h probable maximum precipitation (PMP_{24}) was investigated in a part of the Qareh-Su basin located in the Southeast of Caspian Sea. So far, there have been no estimates of the hydrometeorological PMP values under climate change conditions in the study area. For this purpose, the climatic data were applied during the years 1988–2017. To generate future data, the outputs of the CanESM2 (Second Generation Canadian Earth System Model) model as a general circulation model (GCM) under optimistic (RCP2.6), middle (RCP4.5), and pessimistic (RCP8.5) emission scenarios, and statistical downscaling model (SDSM) were used in the near (2019–2048) and the far (2049–2078) future periods. The PMP_{24} values were estimated using a physical method in the baseline and future periods under the three scenarios. The PMP_{24} value was estimated about 143 mm for the baseline period, using a physical approach. These values were 98, 105, and 109 for the near-future and 129, 122, and 126 mm for the far-future period. The results showed that the physical approach's PMP_{24} values tend to fall at 14–38%. Overall, the PMP_{24} values decrease in the future, and the rate of PMP decrease in the near-future was more than the rate of the far-future. The spatial distribution maps of PMP_{24} in the baseline and future periods showed that the PMP_{24} values decreased from west to east.

Keywords Extreme events · Widespread storms · Maximum 24-h precipitation · Climate scenarios · Flood

1 Introduction

Intensive rainfall and heavy floods are the most catastrophic natural hazards that have enormous social consequences for communities worldwide. In Iran, flood is one of the most devastating natural hazards that occur frequently (Shaffie et al. 2019). The Caspian Sea

✉ Alireza Faridhosseini
farid-h@um.ac.ir

Extended author information available on the last page of the article

region, particularly in Golestan Province, has experienced many heavy flood events. The worst and catastrophic flood occurred in August 2001, in which many people have died. Another massive flood occurred in March 2019, which resulted in an extensive inundation of lowlands. These events were the apparent evidence of climate change created due to human intervention in nature in the last decades (Sharifi et al. 2012; Gharibreza 2019).

Flood risk management is required to decrease the devastating effects of these phenomena. One of the crucial components in flood risk management is probable maximum flood (PMF) estimation. Hydrologists use PMF to design hydrologic infrastructure types in a given basin, such as significant spillways, dam storage capacity, and flood protection structures. To calculate PMF accurately, it is necessary to calculate the probable maximum precipitation (PMP) (Liu et al. 2018). PMP has been defined as "the greatest depth of precipitation for a certain duration meteorologically possible for a given size storm area at a specific time of year (WMO 1986, 2009)".

The World Meteorological Organization has widely proposed statistical and hydrometeorological (physics-based) approaches for estimating PMP (WMO 2009). A statistical approach is a probabilistic procedure that requires a statistical analysis based on the extreme historical precipitation at the meteorological stations where at least 30 years of daily data are available. Several statistical approaches have been used to derive PMP, such as Hershfield method (Hershfield 1961, 1965), multifractal (Douglas and Barros 2003), traditional frequency analysis methods or different statistical distributions such as the generalized extreme value (GEV) (Vivekanandan 2015; Deshpande et al. 2008) and Fisher–Tippett and beta distributions (Nobilis et al. 1991).

Hydro-meteorological estimation approaches can usually be divided into various methods, such as (a) the storm model approach, (b) the generalized method, (c) the moisture maximization method, and (d) the storm transportation method. More details about these methods were mentioned in Rezacova et al. (2005), Rakhecha and Singh (2009), WMO (2009), Collier and Hardaker (1996), Beauchamp et al. (2013), Rakhecha et al. (1995), Papalexiou and Koutsoyiannis (2006), Casas et al. (2011), Micovic et al. (2015), Rouhani and Leconte (2016). However, based on the comparison of studies, there are no generally recommended approaches for PMP estimation (WMO 2009).

There have been several studies about PMP estimation using the hydro-meteorological and statistical approaches in different parts of Iran (Ghahraman 2008; Naseri Moghaddam et al. 2009; Fattahi et al. 2010; Shirdeli 2012), whereas there have been few efforts to investigate climate change's impact on Iran's PMP values in recent years.

Naseri Moghadam et al. (2009) estimated a 1-day PMP for 23 meteorological stations in four central provinces of Iran using the Hershfield method. Their emphasis was to correct the frequency factor of this method for these stations. Their results indicated that the highest value of the frequency factors was 7.6. In another study, Soltani et al. (2014) estimated PMP using statistical and physical approaches for the central regions of Iran. They observed that PMP estimated using the statistical approach was more significant than estimated using the physical approach.

Despite several studies on PMP estimates in Iran, there are just two studies about the Investigation of climate change impacts on PMP values for different regions of Iran. Afrooz et al. (2015) investigated the effects of climate change on PMP in the southern part of Iran using the outputs of two global circulation models (HadCM3 and CGCM3) under A2 emission scenario utilizing three statistical downscaling methods, namely Change Factor (CF), Statistical Downscaling Model (SDSM), and Long Ashton Research Station Weather Generator (LARS-WG). This study used the statistical method to estimate the PMP in the baseline (1971–2000) and the future (2011–2040) periods. Their results showed that PMP

amounts increased up to 18.2 and 27.3%, respectively, by different study areas. Ramak et al. (2017) investigated the climate change impacts on PMP under three scenarios (A1B, A2, and B1) in the Karun catchment (located in the southwest of Iran). It is established that the PMP values for 24, 48, and 72 h are 127, 170, and 185 mm, respectively. The results demonstrated that the PMP value would decrease by up to 5% under the A1B scenario and increase by up to 5% and 10% under A2 and B1 scenarios. Lee et al. (2017) suggested a method to calculate the extreme precipitation in Korea using the Weather Research and Forecasting (WRF) model as a regional climate model. They determined the extreme historical precipitation, reconstructed this event using the WRF model, and then calculated PMP (RCM-PMP). Finally, their results revealed that there is a good agreement between RCM-PMP and existing PMP. In the other research, Lee and Kim (2018) investigated the impact of climate change on future PMPs in Korea using the outputs of three regional climate models provided by CORDEX under RCP scenarios. Their results showed that future PMPs in Korea would have ascending trend, but future PMPs' spatial distribution will be similar to the present.

The Caspian Sea and the ranges of Alborz Mountain are geographical phenomena in the north of Iran that affect rainfall in the southern parts of the Caspian Sea, including the Qareh-Su basin. Furthermore, due to climate change's impacts on extreme precipitation and floods across the study area, hydraulic structures' safety and security would be affected. Therefore, the design rainfall must evaluate under various future climate conditions to design and assess large hydraulic structures. Although the values of PMP_{24} were estimated over the Qareh-Su basin using the statistical and physical method by Afzali-Gorouh et al. (2018), owing to the importance of the climate change impacts on PMP and our literature review, it was determined that so far, there are no studies with emphasis on climate change impact on hydrological (physical) PMP values that have been conducted in the study area. Therefore, this study will analyze the effects of future climate change conditions on the PMP over the north of Iran. Thus, the present study was undertaken to achieve the following objectives:

1. to provide the selected storm rainfall spatial distribution maps for the baseline and the future periods,
2. to produce the DAD curves and the storm maximization factors for the baseline and the future periods,
3. to estimate the 24-h PMP (PMP_{24}) and to assess the behavior of the PMP in response to changing climate conditions.

2 Materials and methods

2.1 Study area and datasets

Iran is located in the southwest of Asia. It is a mountainous country where two major mountain chains, the Alborz Range and the Zagros Range, dissect the country into climactic zones. The Caspian Sea is situated in the northern sector, providing maritime influences. Qareh-Su basin is located between longitudes 54°02′04″ to 54°42′57″ E and latitudes 36°59′29″ to 36°36′54″ N in the southeastern parts of the Caspian Sea covering approximately 1760 km^2 and has an altitude range from −84 to 3221 m. Based on De Martonne's classification, this area is contained sub-humid–warm, humid–moderate,

and sub-humid–moderate climates based on Extended De Martonne classification (Rahimi et al. 2013). This area experiences heavy rainfalls and floods (Afzali-Gorouh et al. 2018). Figure 1 shows the elevation variations, study area, and location of study stations. Geographical and meteorological characteristics of the study stations and their climates based on Extended De Martonne classification are shown in Table 1.

To estimate the PMP under climate change situations, three types of inputs were required. These include observed data (predict and data), National Centre for Environmental Prediction (NCEP) reanalysis (predictor data), and CanESM2 model data from the AR5 for the historical and 2006–2100 for the future period. Although it is generally recommended to use multiple GCMs while studying the potential future change in the climate (Hayhoe et al. 2017), due to time limitations, this study included only one model (CanESM2). The model used in this study is the second-generation Canadian Earth System Model (CanESM2) developed by the Canadian Centre for Climate Modeling and Analysis (CCCma) of Environment Canada (Mesbahzadeh et al. 2019). The primary reason behind using this model in this study is that it is the only model that made daily predictor variables available to be directly fed into SDSM (Hayhoe et al. 2017). World Meteorological

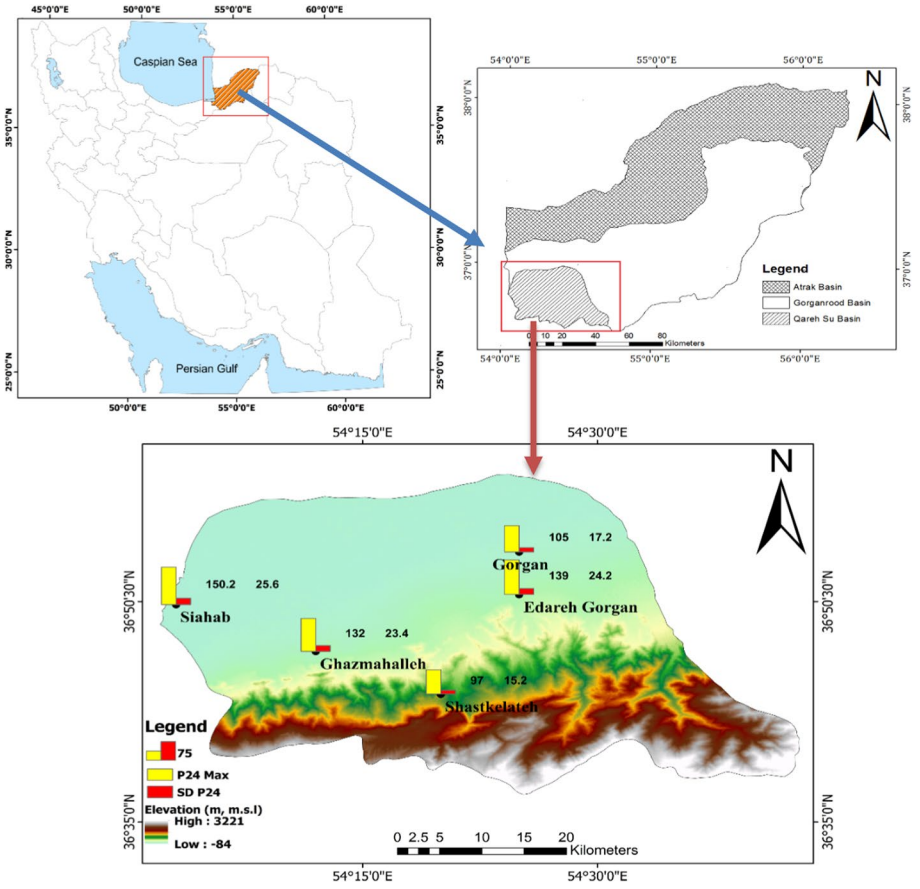

Fig. 1 The elevation variations, geographical location, and maximum and standard deviation of 24-h precipitation of the study stations

Table 1 Geographical and climatological characteristics of the study stations and their climates during the period of 1988–2017

Station	Latitude (N)	Longitude (E)	Elevation (m)	24-h precipitation (mm)				Climate classification Based on Extended De Martonne Classification
				Max	Avg	Min	SD	
Edareh Gorgan	36° 51′	54° 25′	75	139	47.3	17	24.2	Sub-humid–warm
Ghazmahalleh	36° 47′	54° 12′	6	132	54.4	21	23.4	Sub-humid–warm
Shastkelateh	36° 44′	54° 20′	150	97	51.3	25	15.2	Humid–moderate
Gorgan	36° 54’	54° 25’	13.3	105	50.9	28.8	17.2	Sub-humid–warm
Siahab	36° 50′	54° 03′	− 26	150.2	53.6	20.4	25.6	Sub-humid–moderate

Organization (WMO 1988) recommended 30 years or more as a standard reference for climate change and climate variability studies or trends in climatology. Future model change in climate is estimated using the climatological baseline period as a reference period (Houghton et al. 2001). Therefore, the long-term daily and hourly meteorological data from four rain gauge stations (Edareh Gorgan, Ghazmahalleh, Shastkelateh, Siahab) and one synoptic station (Gorgan) during the years 1988–2017 were applied to calculate PMP_{24} and the assessment of climate change impacts on PMP_{24}. These data include three-hour dew point temperature, three-hour wind speed and direction at 10 m elevations, three-hour and monthly air pressure, and 3- and 24-h precipitation. We gathered these data from the IRIMO (Islamic Republic of Iran Meteorological Organization 2018).

As mentioned above, to investigate climate change impact on PMPs, two series of daily predictors were used: the first, the 26 predictors of the National Center for Environmental Prediction (NCEP), which will obtain from the statistical downscaling model (SDSM) website (http://co-public.lboro.ac.uk/cocwd/SDSM/data.html), and second (b) the 26 predictors of CanESM2, obtained from the Canadian website (http://www.cccsn.ec.gc.ca/?page=pred-canesm2). These databases were specifically processed for SDSM. During the arrangement, the NCEP predictors ($2.5° \times 2.5°$) were first interpolated to the grid resolution of CanESM2 ($2.8° \times 2.8°$) to remove the spatial incoordination. The predicted data were acquired by downscaling the CanESM2 model under three RCP scenarios using the SDSM for each study station detailed in Sect. 2.4. Table 2 shows the characteristics of the used climate model.

2.2 Physical approach

There are two common physical approaches, namely the mountainous and convergence models, to calculate PMP (Joos et al. 2005). The convergence model is based on physical storm characteristics, i.e., dew point temperature, wind speed, wind direction, etc. The main steps to calculate PMP using the convergence model are selecting severe storms, producing the depth-area-duration (DAD) curves, moisture maximization, and wind maximization. The flowchart of the methodology for the physical approach is mentioned in Fig. 2.

2.2.1 Selection of the most severe and widespread storms

A severe and widespread storm is a weather condition that produces precipitation in all basins and even around the basin. The most severe and widespread storms are selected based on maximum discharge and maximum 24-h rainfall data.

2.2.2 Producing DAD curves

The spatial distribution of rainfall rarely is uniform over a region; in the center of the storm, the depth of rainfall is maximum. DAD curves are essentially used to prove that as the distance from the center of the storm increases, the depth of precipitation decreases. Indeed, DAD curves are a suitable tool to demonstrate the spatial distribution of rainfall over a basin or large region. Therefore, the procedure for obtaining DAD curves is described below:

1. Determination of the day of highest average rainfall depth,

Table 2 The characteristics of CanESM2 model Arora et al. (2011)

Category	Model name	Resolution (longitude × latitude)		Resolution (temporal)	Institute	Scenarios
		Atmosphere	Ocean			
GCM	CanESM2	2.8° × 2.8°	1.41° × 0.94°	Daily	Canadian Center for Atmospheric Research, Canada (CCCMA)	RCP2.6, RCP4.5, RCP8.5

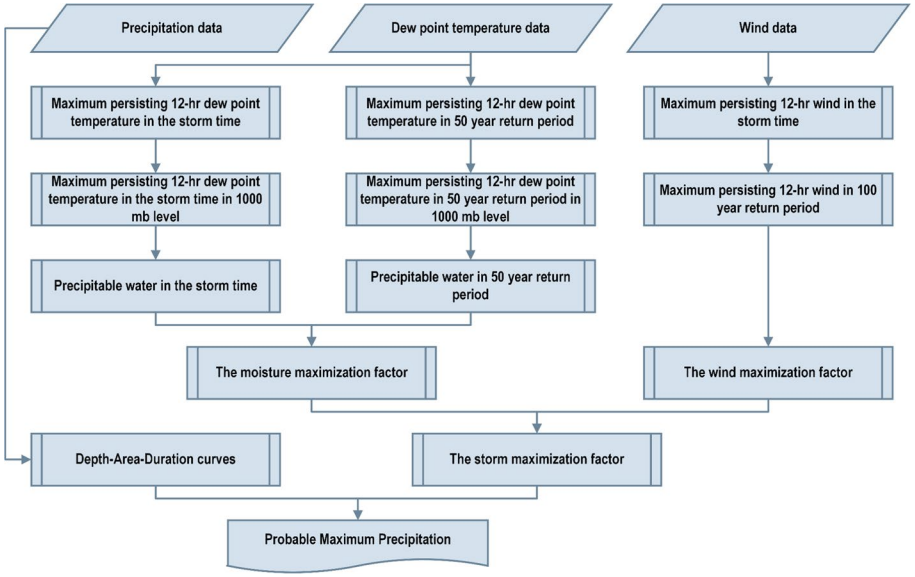

Fig. 2 The flowchart of the methodology for the physical approach (Source: own elaboration)

2. Producing isohyets maps which is one of the main steps in the preparation of DAD curves,
3. Calculation of the enclosed area between two isohyets,
4. Calculation of the incremental volume of rainfall through the multiplication of the area between the two isohyets and the average of the two isohyet values,
5. Calculation of the total volume of rainfall,
6. Computation of the average depth of rainfall over the study area through dividing the total volume of rainfall by the total area
7. Plotting the highest average depths for different areas as DAD curve (Raghunath 2006).

Using an analysis of the storms, DAD curves can be obtained. DAD curves are also applied to generalized relations for other areas or other basins with similar climate and topographic characteristics. The first step to developing the DAD curve is collecting the precipitation data for all storm areas.

2.2.3 Storm maximization

The storm maximization factor is calculated by the moisture maximization factor multiplied by the wind maximization factor. The moisture maximization method is an acceptable procedure to maximize the rainfall values associated with severe storms (Rakhecha and Singh 2009). This method assumes that the atmospheric moisture would hypothetically rise to a high value that is regarded as the upper limit of moisture. The mentioned limit is estimated from historical records of dew point temperature. After selecting severe and widespread storms and calculating the average rainfall depth for the study area, it is necessary to calculate the maximum humidity source in order to maximize selected storms. By converting mean monthly pressure data at each station to 1000-mb pressure level, the effect of topography could be ignored. Dew point temperature and maximum 12-h persisting

condition at the stations during all storm events were computed and reduced to equivalent mean sea level (MSL, i.e., 1000-mb pressure level). The moisture maximization factor (*FM*) is calculated by Eq. (1).

$$\mathrm{FM} = \frac{W_{\mathrm{m}}}{W_{\mathrm{s}}}, \tag{1}$$

where W_{m} is the maximum precipitable water in the 1000 to 200 mb levels, which can be obtained based on the maximum 12-h duration dew point with 50-year return period. W_{s} is the maximum precipitable water at 1000 to 200 mb levels, which can be obtained based on maximum 12-h duration dew point in a simultaneous period with the storm (WMO 2009). Wind maximization is most commonly used in orographic regions when it appears that observed storm rainfall over a mountain range might vary in proportion to the speed of the moisture-bearing wind blowing against the range. The wind maximization ratio is simply the maximum average wind speed ratio for some specific duration and critical direction obtained from a long record of observations, e.g., 50 or 100 years, to the observed maximum average wind speed for the same duration and direction in the storm being maximized. The wind speed maximization factor (MW) is defined by Eq. (2).

$$\mathrm{MW} = \frac{\mathrm{MW}_1}{\mathrm{MW}_2}, \tag{2}$$

where MW_1 and MW_2 are the maximum wind speed with 100-year return period and the maximum persisting 12-h wind speed during the storm, respectively (WMO 2009). Finally, PMP is determined by the precipitation depth (*R*) multiplied by moisture maximization and wind maximization factors based on Eq. (3).

$$\mathrm{PMP} = \mathrm{FM} \times \mathrm{MW} \times \mathrm{R}. \tag{3}$$

2.3 RCP scenarios and the statistical downscaling model (SDSM)

According to the Fifth Assessment Report of the Intergovernmental Panel on Climate Change (AR5), the future climate condition at the global scale is simulated using general circulation models (GCM). Based on the AR5 models, that was prepared using the output of the CMIP5 models, the surface temperature at the end of the twenty-first century will increase more than 1.5 °C (IPCC 2014). The AR5 models use representative concentration pathways (RCPs) emission scenarios that have four pathways including RCP2.6, RCP4.5, RCP6, and RCP8.5, based on their radiative forcing values in 2100 (Van Vuuren et al. 2011; Moss et al. 2010). For instance, RCP2.6 is a pathway where radiative forcing peaks at about 3 W m^{-2} before 2100 and then reduces. The general circulation model (GCM) is the most suitable method for assessing the impacts of climate change on global environmental systems (Sehgal et al. 2018), but due to their coarse grid spacing (about 10 km), the application of these models is not appropriate at regional or local scales (Hay et al. 2000; Gebremeskel et al. 2005). Downscaling is the most important and suitable tool for linking the local/regional scale and GCM. As a whole, there are two statistical and dynamic methods for downscaling GCM (Salehnia et al. 2019). Dynamical downscaling methods are more complicated and require more computational demand, whereas statistical methods do not need expensive requirements, such as several cores, and many hours to run with computers. (Trzaska and Schnarr,

2014). In the SDSM, as a widely used statistical downscaling method, the empirical/statistical relationship between large-scale and local/regional climate variables is established (Wilby et al. 2002; Palatella et al. 2010; Huang et al. 2011). The SDSM, which is developed by Wilby et al. (2002), is a useful tool that combined multiple linear regression and stochastic weather generators (Dehghan et al. 2020), and users are permitted to simulate, series of daily climatic data for present and future periods by obtaining statistical parameters from observed data series (Gagnon et al. 2005). The stochastic component of SDSM allows the generation of 100 daily simulations that have good correlation with observed data in the validation step (Gagnon et al. 2005). Based on the type and nature of the input data, SDSM is calibrated under conditional and unconditional process. Hence, precipitation and temperature are conditional and unconditional processes, respectively (Gebrechorkos et al. 2019). The method has four main steps including the screening of NCEP predictors, calibration, validation, and climate scenario generation under the RCP scenarios for future time horizons. The flowchart and detail of methodology for downscaling and Climate scenario generation via SDSM are described in Dehghan et al. (2020).

2.3.1 The screening of NCEP predictors

Recognizing empirical relationships between NCEP predictors and predictands is important to all statistical downscaling methods and is often the most time-consuming step in the process. The purpose of this step is to help the user in the selection of suitable downscaling predictor variables for model calibration (Wilby and Dawson 2007). In this step, due to the correlation matrix, partial correlation, and P-value, NCEP predictors are selected based on strength of each predictor–predictand relationship. These indicators have used in Dehghan et al. (2020), Al-Mukhtar and Qasim (2019), and Mahmood and Babel (2014).

2.3.2 Calibration and validation

In this step, monthly regression models are produced using selected NCEP predictor variables and a simulation is executed using a part of input data series. The quality of model calibration is reported using monthly average of coefficient of determination (R^2; Eq. 4) and values of standard error (SE; Eq. 5). The other parts of input data series are simulated with the calibrated regression models. Then, the predicted and observed monthly means and variances are compared using R^2 and F-tests, respectively.

$$R^2 = \frac{\left[\sum_{i=1}^{n}\left[O_i - \bar{O}_i\right].\left[P_i - \bar{P}_i\right]\right]^2}{\sum_{i=1}^{n}\left[O_i - \bar{O}_i\right]^2.\sum_{i=1}^{n}\left[P_i - \bar{P}_i\right]^2}, \tag{4}$$

$$\mathrm{SE} = \frac{\sigma}{\sqrt{n}}, \tag{5}$$

where O_i and P_i were the observed and predicted values, $\overline{O}_i$ and $\overline{P}_i$ were the average of observed and predicted values, σ was sample standard deviation, and n is the number of samples.

2.3.3 Climate scenario generation

After validation, the daily time series of dew point temperature and precipitation were generated for future time horizons including under RCP scenarios.

2.4 Performance criteria

The performance and accuracy of the model compared the generated future climatic data with observed data were judged by four performance criteria including coefficient of determination "R^2", root mean square error "RMSE" (MacLean 2005), mean absolute error "MAE" (MacLean 2005), and Nash and Sutcliffe efficiency "NSE" (Nash and Sutcliffe 1970) that are defined as:

$$\mathrm{RMSE} = \sqrt{\frac{\sum_{i=1}^{n}\left[O_i - \bar{P}_i\right]^2}{n}}, \tag{6}$$

$$\mathrm{MAE} = \frac{\sum_{i=1}^{n}\left|O_i - P_i\right|^2}{n}, \tag{7}$$

$$\mathrm{NSE} = 1 - \frac{\sum_{i=1}^{n}\left[O_i - P_i\right]^2}{\sum_{i=1}^{n}\left[O_i - \overline{O}_i\right]^2}. \tag{8}$$

R^2 varies between 0 and 1 and a value of R^2 closer to 1 shows better performance. RMSE reveals the actual division among the predicted and observed values. Also, RMSE value is closer to or equal to zero, and smaller value of MAE reveals a more accurate performance. The NSE values ranged from $-\infty$ to 1, and the value of 1 shows perfect fit.

3 Results and discussion

3.1 SDSM calibration and validation

As mentioned in the previous sections, SDSM was applied to downscale rainfall and dew temperature from GCMs. To this end, the precipitation data of five stations including Edareh Gorgan, Ghazmahalleh, Shastkelateh, Gorgan, and Siahab, and the dew point temperature data of one synoptic station named Gorgan were used as predictand data. During the screening process, the NCEP predictors were determined with mean absolute partial correlation, the correlation matrix, and *P*-value, for dew point temperature and rainfall with a confidence level of 95%. Table 3 illustrates the combination of selected NCEP predictors for each predictand to improve the performance of SDSM during calibration in the study stations.

During calibration step, two indicators _ monthly R^2 and SE_ were applied to control the model performance and efficiency. Monthly R^2 values were calculated for each station and vary from 0.275 to 0.37 for rainfall (Table 4); also, the monthly R^2 value was 0.7 for

Table 3 Selected predictors for dew point temperature and rainfall during screening of predictors step, in the Qareh-Su basin

Variable	Stations	The selected NCEP predictors
Rainfall	Edareh Gorgan	p5_v, shum
	Ghazmahalleh	p8_z, p850
	Shastkelateh	p500, p8_f
	Gorgan	p850, p_zh
	Siahab	mslp, p_u, p5_v
Dew point temperature	Gorgan	p_u, p5_f, shum, temp

p5_v meridional velocity component at 500 hPa, *shum* near-surface specific humidity, *p8_z* vorticity at 850 hPa, *p850* 850 hPa geopotential height, *p500* 500 hPa geopotential height, *p8_f* geostrophic airflow velocity at 850 hPa, *p_zh* divergence near the surface, *mslp* mean sea level pressure, *p_u* zonal velocity component near the surface, *p5_f* geostrophic airflow velocity at 500 hPa, *temp* near-surface air temperature

Table 4 The results of model calibration

Variable	Stations	Calibration period	Monthly average of R^2	SE
Rainfall	Edareh Gorgan	1988–2002	0.313	0.365
	Ghazmahalleh	1988–2002	0.37	0.385
	Shastkelateh	1988–2002	0.29	0.354
	Gorgan	1988–2002	0.275	0.39
	Siahab	1988–2002	0.37	0.37
Dew point temperature	Gorgan	1988–2002	0.7	1.6

dew point temperature. The maximum and minimum values of SE, for rainfall, were 0.39 and 0.354, which is related to Shastkelateh and Gorgan stations, respectively. The SE value for dew point temperature was 1.6.

As you know, precipitation downscaling is necessarily more problematic than temperature, because daily precipitation amounts at individual sites are relatively poorly resolved by regional-scale predictors, and because precipitation is a conditional process (i.e., both the occurrence and amount processes must be specified). Therefore, due to the high variation of rainfall data, its correlation coefficient is always lower than the correlation coefficient of air temperature data. There are some articles such as Wilby and Dawson (2004) that downscaled the rainfall data of Blogsville with four predictors including p_v, p_z, p500, and shum with $R^2 = 0.1$. In the other study, the amounts of R^2 in the calibration and validation steps were 0.25–0.49 and 0.15–0.35, respectively (Emami and Koch 2018). In the present study, during the screening process, the best NCEP predictors were selected and the calibration and validation of the model were applied based on the best NCEP predictors.

Based on Table 4, monthly average R^2 for the rainfall data in the validation stage was lower than the dew point temperature data and the efficiency of the SDSM model in downscaling the rainfall data for all stations are similar.

After successful validation, the daily time series of dew point temperature and rainfall were generated using SDSM model and the outputs of CanESM2 for two time horizons including the near-future (2019–2048) and the far-future (2049–2078), under three RCP scenarios (RCP2.6, RCP4.5, and RCP8.5). Table 5 summarizes the statistical comparison of the projection data and observed data in calibration and validation steps. The NSE and R^2 values show the high accuracy of downscaling dew point temperature and rainfall data. Therefore, SDSM model can be used to estimate future values of rainfall and dew point temperature.

According to Fig. 3a, which shows the variation of the monthly and seasonal dew point temperature of Gorgan station during future periods, in the near-future period, for RCP2.6 and 4.5, monthly average dew point temperature decreased from March to May, and for RCP8.5 fell in April and May. In contrast, other months show dew point temperature increases in all scenarios. The maximum and minimum percent of increasing dew point temperature is equal to 67% related in January under RCP8.5 and 1% related in June under RCP4.5. The seasonal average dew point temperature during the near-future period increased in winter, summer, and autumn under three RCP scenarios. The average observed dew point temperature was more significant in the spring than the average future dew point temperature under three RCP scenarios. The maximum dew point temperature increase was equal to 15% in the seasonal time scale, related in autumn under RCP4.5 and RCP 8.5. In addition, the minimum dew point temperature increase was equivalent to 10%, related in summer under RCP4.5. During the far-future period, monthly average dew point temperature decreased about 1% in April under RCP4.5. In other months and RCPs, monthly average dew point temperature increased between 0.3 and 67%, related in April and May under RCP2.6 and January under RCP 8.5, respectively. The maximum dew point temperature increase in the seasonal time scale was equal to 37%, related in winter under RCP8.5. Also, the minimum dew point temperature increase was equal to 3%, related in spring under RCP4.5.

The variation of the monthly and seasonal rainfall of Gorgan station during the future periods is shown in Fig. 3b. Overall, the monthly variation of rainfall in Gorgan station in the near-future was decreased except August and September under RCP 4.5 and September under RCP8.5. These values were 11, 1, and 8%, respectively. Also, the maximum values of monthly decrease were 30, 60, and 65% in RCP2.6, RCP4.5, and RCP8.5, which are related in June, July, and April, respectively. The minimum rainfall decreases were 4% under RCP 2.6 (November) and 1% under RCP4.5 (April) and RCP8.5 (August). The seasonal average rainfall during this period decreased for all seasons and all RCPs. Besides, in the far-future period, the values of monthly rainfall decreases were 38, 54, and 65% related in May, December, and April, under RCP2.6, RCP4.5, and RCP8.5, respectively. Also, these seasonal values decreased under all RCPs. This is consonant with the results of Abdolhosseini et al. (2012), indicating that the rainfall tended to reduce under climate change conditions. It should be noted that they used the SDSM and the outputs of the HadCM3 climate model under A2 scenario to estimate the potential evapotranspiration in the Qareh-Su basin.

3.2 PMP calculation using physical method

The observed and the future rainfall data were used to determine the most severe and widespread storms. Based on these data, thirteen storms were selected as the most severe and widespread storms during the baseline, near, and far-future periods (Table 6).

Table 5 Model performance evaluation in validation and projection of the baseline period

Variable	Stations	Validation					Projection				
		R^2	Significant level of F test	RMSE	MAE	NSE	R^2	Significant level of F test	RMSE	MAE	NSE
Rainfall	Edareh Gorgan	0.8	4.5×10^{-14}	0.8	0.6	0.7	0.6	0.004	1.4	1.1	0.08
	Ghazmahalleh	0.8	2.4×10^{-16}	1.3	1.0	0.3	0.4	0.02	1.9	1.7	0.02
	Shastkelateh	0.8	6.5×10^{-15}	1.2	0.9	0.5	0.3	0.09	2.09	2.3	0.06
	Gorgan	0.8	1×10^{-4}	1.1	0.8	0.4	0.5	0.008	1.5	1.6	0.07
	Siahab	0.8	2.1×10^{-12}	1.3	1.2	0.5	0.3	0.07	2.49	2.1	0.05
Dew point temperature	Gorgan	0.9	7.5×10^{-14}	0.6	0.5	0.9	0.9	9.8×10^{-14}	1.1	0.8	0.9

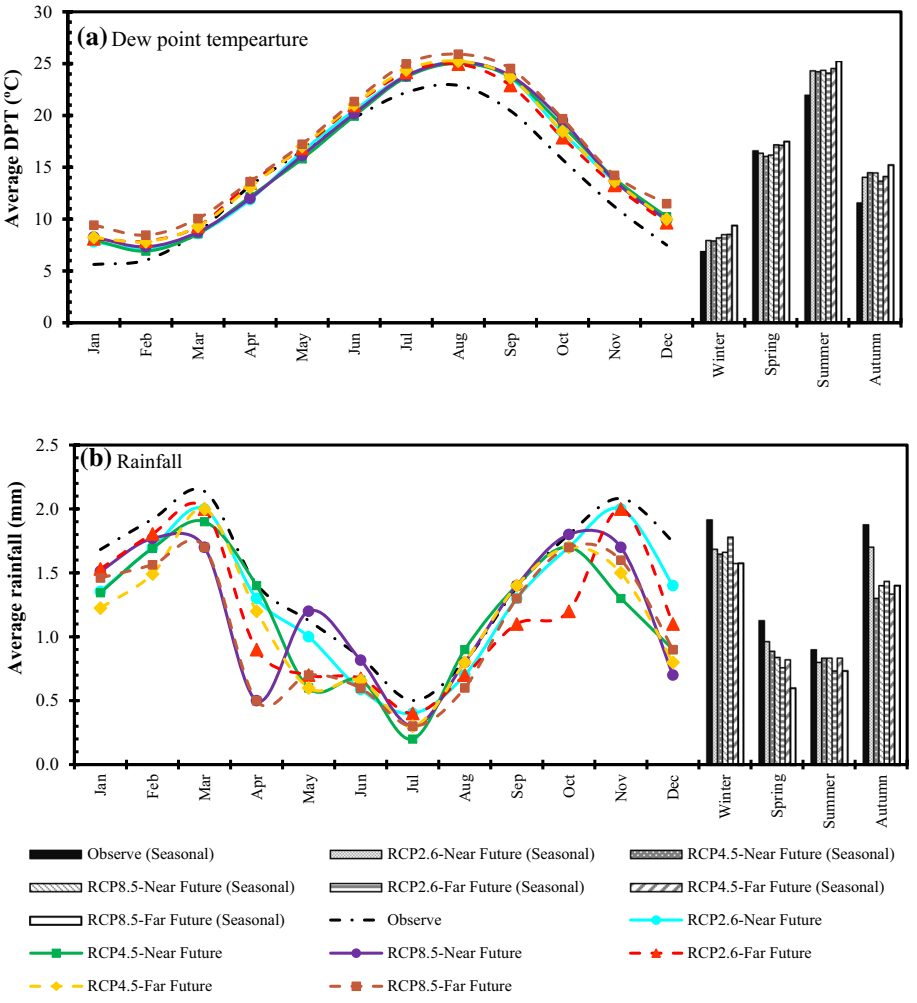

Fig. 3 The variation of the monthly and seasonal **a** dew point temperature and **b** rainfall of Gorgan station during future periods

After determination of the most severe and widespread storm dates, in order to analyze and the spatial distribution of rainfall and drawing the isohyet maps, rainfall gradient (elevation–rainfall relationship) was investigated. Investigation of rainfall–elevation relationship showed that there is no significant correlation between rainfall and elevation at the 5% level of significance. Therefore, isohyet maps with 10-mm interval for each storm were developed using inverse distance weighting (IDW) method through ArcMap version 10.5; also, the enclosed area between two isohyets was measured. Finally, DAD curves for each storm during baseline and two future periods under three RCP scenarios were generated. Table 7 shows the required calculations to produce DAD curves.

DAD's envelope curves were produced to select the highest depths of rainfall in each scenario and each period. Figure 4 shows the DAD curves for storms chosen in the near-future period under RCP8.5 scenario. Based on this figure, the storm of September 2025

Table 6 Dates of 24-h duration severe and widespread storms in the study area during the baseline, the near and the far-future periods under the RCP scenarios

No.	Baseline (1988–2017)	Near-future (2019–2048)	Far-future (2049–2078)
	Date of occurrence (mm/dd/yyyy)	Date of occurrence (mm/dd/yyyy)	Date of occurrence (mm/dd/yyyy)
1	11/12/1995	09/27/2045	09/30/2064
2	10/29/1993	04/25/2044	11/11/2062
3	10/09/2006	05/11/2025	10/06/2059
4	07/17/2012	03/14/2023	10/06/2057
5	01/11/2013	05/11/2040	10/23/2060
6	09/29/2008	09/14/2019	01/30/2051
7	09/27/1995	05/19/2031	03/10/2066
8	10/13/1991	04/26/2027	10/24/2078
9	10/21/2011	02/27/2040	03/30/2065
10	10/13/2012	05/09/2034	10/24/2074
11	08/16/1993	02/02/2026	04/21/2053
12	12/26/2005	10/21/2048	02/05/2051
13	06/04/2014	09/12/2025	10/05/2059

Table 7 The average of 24-h rainfall for the storm of September 12, 2025, in the study area

Limit of isohyet lines (mm)	Average of isohyet (mm)	Area (km^2)	Cumulative area (km^2)	Volume of the rainfall (1000 m^3)	Cumulative volume of the rainfall (1000 m^3)	Average of maximum rainfall (mm)
90–80	85	14.11	14.11	1199.4	1199.4	85.0
80–70	75	26.41	40.5	1980.8	3180.2	78.5
70–60	65	36.41	76.9	2366.7	5546.8	72.1
60–50	55	58.31	135.2	3207.1	8753.9	64.7
50–40	45	123.31	258.6	5549.0	14,302.8	55.3
40–30	35	227.12	485.7	7949.2	22,252.0	45.8
30–20	25	456.91	942.6	11,422.8	33,674.8	35.7
30–10	15	464.21	1406.8	6963.2	40,637.9	28.9
10–0	5	353.21	1760.0	1766.1	42,404.0	24.1

was the most severe and widespread one, which was considered as the envelope curve. In this curve, maximum rainfall value was 85 mm, which indicated the storm center. As the distance from the center of the storm increases, the depth of precipitation decreases, because the area affected by the storm increases.

The moisture maximization factor (W_m) was calculated through maximization of dew point temperature data with 50-year return period using Tephigram (Skew-T diagram). Besides, the wind maximization factor (MW_1) was estimated using wind speed data of Gorgan station with 100-year return period. Because wind is a vector variable and projection of its behavior for future periods using statistical methods is associated with many

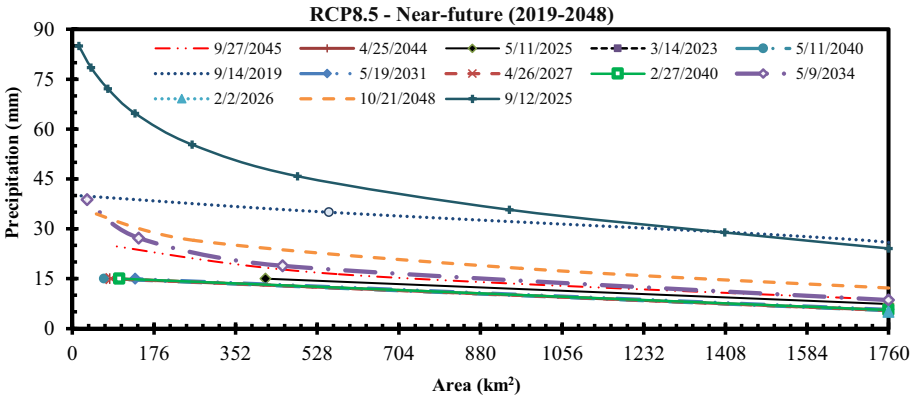

Fig. 4 Depth–area–duration curves for selected storms in near-future period under RCP8.5 scenario

uncertainties, wind maximization factor of baseline period is used for maximizing storms in the future periods. After the calculation of moisture and wind maximization factors, PMP is calculated using Eq. 5. The amounts of moisture and wind maximization factors are shown in Table 8.

Figure 5 shows the PMP values for the baseline and the future periods under the RCP scenarios. The PMP value for the baseline period is 143 mm (Afzali-Gorouh et al. 2018). Under changing climatic conditions, the PMP values will decrease. For the near-future, the PMP values are 98, 105, and 109 mm under the RCP2.6, RCP4.5, and RCP8.5, respectively. For the far-future, these values are 129, 122, and 126 mm under RCP2.6, RCP4.5, and RCP8.5, respectively. The results showed that PMP values would decrease in future periods, but the near-future reduces more than the far-future.

The percentage of PMP differences between the baseline and the near-future period will be 21, 26, and 24% in RCP2.6, RCP4.5, and RCP8.5 scenarios, respectively. These mentioned values will be 10, 15, and 12% in the far-future period. These values showed that the PMP values would decrease in future periods under climate change conditions. According

Table 8 The maximization factors, PMP values, and percentage of differences between the baseline and the future periods under the RCP scenarios

Period	Scenario	Date of occurrence (mm/dd/yyyy)	Maximum persisting 12-h dew point in 1000 mb level (°C)		Maximum persisting 12-h wind (Knot)		Maximization factor	
			In the storm time	50-year return period	In the storm time	100-year return period	FM	MW
1988–2017	Baseline	10/29/1993	14.1	20.6	7	10.1	1.4	1.4
2019–2048	RCP2.6	02/02/2026	3.7	14.3	9.7	19.2	2.1	1.98
	RCP4.5	02/02/2026	5.8	15.3	9.7	19.2	1.8	1.98
	RCP8.5	02/02/2026	4.6	14.9	9.7	19.2	1.9	1.98
2049–2078	RCP2.6	01/30/2051	8.7	17.2	8.3	16.6	1.8	2.0
	RCP4.5	01/30/2051	10.8	17.8	8.3	16.6	1.6	2.0
	RCP8.5	01/30/2051	8.9	18.0	8.3	16.6	1.9	2.0

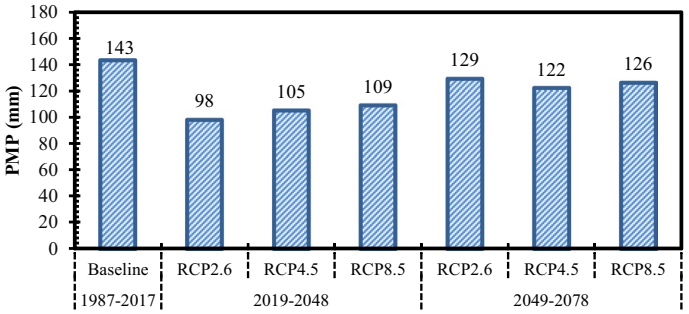

Fig. 5 The PMP values and percentage of differences between the baseline and the future periods under the RCP scenarios

to Fig. 6, the maximum and minimum PMP24 changing rate during near-future period under RCP2.6, RCP4.5, and RCP8.5 scenarios are equal to 64, 62, 59, and 48, 33, and 24 percent. These values for far-future period are 45, 47, 46, and 13, 17, and 12, respectively. The maximum and minimum ranges of variation are related in RCP8.5 and RCP2.6 during near-future period.

4 Conclusions

PMP projection and investigation of climate change impacts on PMP estimates are two critical issues to calculate the design of floods and dam safety management. The Qareh-Su Basin has experienced heavy floods and rainfalls since it is located beside the Caspian Sea and the air masses bring moisture from the Caspian Sea to this area. Therefore, the impact of climate change on 24-h PMP in this basin was studied using outputs of the general circulation model CanESM2 under three RCP scenarios utilizing the statistical downscaling model (SDSM).

Hence, SDSM was successfully calibrated during the period of 1988 to 2002 and validated during the period of 2003 to 2018 to investigate future changes in PMP_{24} in the

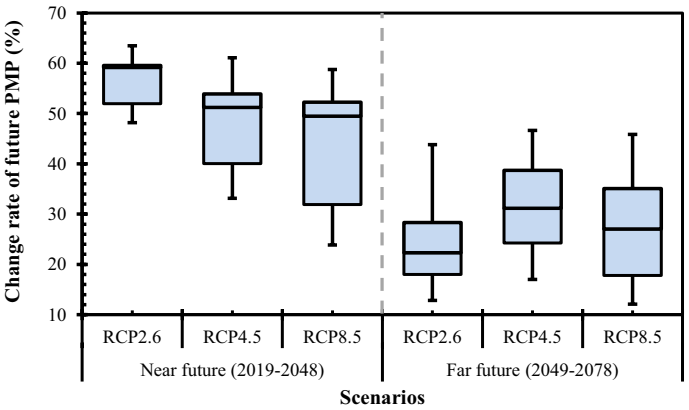

Fig. 6 The change rate of future PMP_{24} in the future periods under RCP scenarios

Qareh-Su basin for the near (2019–2048) and far (2049–2078) future periods under the RCP2.6, RCP4.5, and RCP8.5 scenarios, compared to the baseline period (1988–2018).

In this study, due to the availability of long-term precipitation (in four rain gauge stations) and dew point temperature (one synoptic station) data as well as the presence of several severe and widespread storms in the study area, the physical approach was considered to calculate the PMP_{24}. The results obtained from this approach showed that PMPs would decrease in future periods under all RCP scenarios. The PMP values for the near-future period compared to the baseline period under RCP2.6, RCP4.5, and RCP8.5 scenarios will reduce by 31, 26, and 24%, respectively. For the far-future, under three scenarios will decrease by 10, 15, and 12%, respectively, compared to the baseline period.

Finally, it is recommended that the results of PMP values are estimated and compared with the outputs of other climate models and other downscaling methods.

Author contributions AF and BB conceived of the presented idea. ZA-G developed the theory and performed the computations. NS verified the analytical methods. AM encouraged to investigate and supervised the findings of this work. All authors contributed to the interpretation of the results. ZA-G and NS took the lead in writing the manuscript. All authors provided critical feedback and helped shape the research, analysis and manuscript.

Funding The authors received no financial support for the research, authorship, and/or publication of this article.

Data availability The raw/processed data required to reproduce the above findings cannot be shared at this time as the data also forms part of an ongoing study.

Code availability Not applicable.

Declarations

Conflict of interest The authors declare that there is no conflict of interest.

Ethical approval The data included in this manuscript have not been published previously and are not under consideration by any other journals.

Consent to participate The authors have been participated in the preparation of the manuscript and have given their permission to submit this manuscript with its present format.

Consent for publication The authors have been satisfied in the publication of the manuscript and have given their permission to publish this manuscript with its present format.

References

Abdolhosseini M, Eslamian S, Mousavi SF (2012) Effect of climate change on potential evapotranspiration: a case study on Gharehsoo sub-basin, Iran. Int J Hydrol Sci Technol 2(4):362. https://doi.org/10.1504/ijhst.2012.052373

Afrooz AH, Akbari H, Rakhshandehroo GR, Pourtouiserkani A (2015) Climate change impact on probable maximum precipitation in Chenar-Rahdar River Basin. Watershed Manag 36. https://doi.org/10.1061/9780784479322

Afzali-Gorouh Z, Bakhtiari B, Qaderi K (2018) Probable maximum precipitation estimation in a humid climate. Nat Hazards Earth Syst Sci 18(11):3109–3119

Al-Mukhtar M, Qasim M (2019) Future predictions of precipitation and temperature in Iraq using the statistical downscaling model. Arab J Geosci 12(2):25. https://doi.org/10.1007/s12517-018-4187-x

Arora VK, Scinocca JF, Boer GJ, Christian JR, Denman KL, Flato GM et al (2011) Carbon emission limits required to satisfy future representative concentration pathways of greenhouse gases. Geophys Res Lett 38(5):12. https://doi.org/10.1029/2010GL046270

Beauchamp J, Leconte R, Trudel M, Brissette F (2013) Estimation of the summer-fall PMP and PMF of a northern watershed under a changed climate. Water Resour Res 49:3852–3862. https://doi.org/10.1002/wrcr.20336

Casas MC, Rodriguez R, Prohom M, Gazquez A, Redano A (2011) Estimation of probable maximum precipitation in Barcelona (Spain). Int J Climatol 31:1322–1327. https://doi.org/10.1002/joc.2149

Collier CG, Hardaker PJ (1996) Estimating probable maximum precipitation using a storm model approach. J Hydrol 183:227–336. https://doi.org/10.1016/0022-1694(95)02953-2

Dehghan Sh, Salehnia N, Sayari N, Bakhtiari B (2020) Prediction of meteorological drought in arid and semi-arid regions using PDSI and SDSM: a case study in Fars Province. Iran Arid Land 12(2):318–330. https://doi.org/10.1007/s40333-020-0095-5

Deshpande NR, Kulkarni BD, Verma AK, Mandal BN (2008) Extreme rainfall analysis and estimation of probable maximum precipitation (PMP) by statistical methods over the Indus river basin in India. J Spat Hydrol 8:22–36

Douglas EM, Barros APB (2003) Probable maximum precipitation estimation using multifractals: application in the Eastern United States. J Hydrometeorol 4:1012–1024. https://doi.org/10.1175/1525-7541(2003)004%3c1012:PMPEUM%3e2.0.CO;2

Emami F, Koch M (2018) Evaluation of statistical-downscaling/bias-correction methods to predict hydrologic responses to climate change in the zarrine river basin. Iran Climate 6(2):30. https://doi.org/10.3390/cli6020030

Fattahi E, Noorian AM, Noohi K (2010) Comparison of physical and statistical methods for estimating probable maximum precipitation in south-western basins of Iran. Desert 15:127–132

Gagnon S, Singh B, Rousselle J, Roy L (2005) An application of the statistical downscaling model (SDSM) to simulate climatic data for streamflow modelling in Québec. Can Water Resour J 30(4):297–314. https://doi.org/10.4296/cwrj3004297

Gebrechorkos SH, Hülsmann S, Bernhofer C (2019) Statistically Downscaled Climate Dataset for East Africa Sci Data 6:31. https://doi.org/10.1038/s41597-019-0038-1

Gebremeskel S, Liu YB, de Smedt F, Hoffmann L, Pfister L (2005) Analyzing the effect of climate changes on streamflow using statistically downscaled GCM scenarios. Int J River Basin Manag 2(4):271–280. https://doi.org/10.1080/15715124.2004.9635237

Ghahraman B (2008) The estimation of one-day duration probable maximum precipitation over Atrak watershed in Iran. Iranian J Sci Technol 32:175–179

Gharibreza MR (2019) Huge inundation (March 2019) of Golestan Province, Iran, lessons that we learned. Open Access J Environ Soil Sci 4(3):507–510. https://doi.org/10.32474/OAJESS.2019.04.000188

Hay LE, Wilby RL, Leavesley GH (2000) A comparison of delta change and downscaled GCM scenarios for three mountainous basins in the United States. J Am Water Resour As 36(2):387–397. https://doi.org/10.1111/j.1752-1688.2000.tb04276.x

Hayhoe K, Edmonds J, Kopp RE, LeGrande AN, Sanderson BM, Wehner MF, Wuebbles, DJ (2017) Climate models, scenarios, and projections. In: Climate Science Special Report: Fourth National Climate Assessment, Volume I [Wuebbles, D.J., D.W. Fahey, K.A. Hibbard, D.J. Dokken, B.C. Stewart, and T.K. Maycock (eds.)]. U.S. Global Change Research Program, Washington, DC, pp. 133–160, https://doi.org/10.7930/J0WH2N54.

Hershfield DM (1961) Estimating the probable maximum precipitation. ASCE J Hydraul Eng 87:99–106

Hershfield DM (1965) Method for estimating probable maximum precipitation. J Am Water Works As 57:965–972

Houghton JT, Ding Y, Griggs DJ, Noguer M, Linden PJVd, Dai X, Johonson CA (2001) Climate Change (2001): the scientific basis: contribution of working group I to the third assessment report of IPCC

Huang J, Zhang J, Zhang Z, Xu C, Wang B, Yao J (2011) Estimation of future precipitation change in the Yangtze River basin by using statistical downscaling method. Stoch Env Res Risk As 25(6):781–792. https://doi.org/10.1007/s00477-010-0441-9

IPCC (2014) Summary for policymakers. In: Field CB, Barros VR, Dokken DJ, Mach KJ, Mastrandrea MD, Bilir TE, Chatterjee M, Ebi KL, Estrada YO, Genova RC, Girma B, Kissel ES, Levy AN, MacCracken S, Mastrandrea PR, White LL (eds) Climate change (2014): impacts, adaptation, and vulnerability. Part A: global and sectoral aspects. Contribution of Working Group II to the Fifth Assessment Report of the Intergovernmental Panel on Climate Change. Cambridge and New York: Cambridge University Press, pp 1–32

Islamic Republic of Iran Meteorological Organization (2018) Meteorological data from synoptic station during years 1981–2018. Available at: http://irimo.ir/eng/wd/720-Products-Services.html. Accessed 11 Mar 2018

Joos B, Darakhani J, Mouvet L, Mehinrad A (2005) An integrated probabilistic approach for determining the effects of extreme hydrological events on a flood evacuation system, 73rd annual meeting of ICOLD, Tehran

Lee O, Kim S (2018) Estimation of future probable maximum precipitation in Korea using multiple regional climate models. Water 10:637. https://doi.org/10.3390/w10050637

Lee J, Choi J, Lee O, Yoon J, Kim S (2017) Estimation of probable maximum precipitation in Korea using a regional climate model. Water 9:240. https://doi.org/10.3390/w9040240

Liu T, Liang Z, Chen Y, Lei X, Li B (2018) Long-duration PMP and PMF estimation with SWAT model for the sparsely gauged Upper Nujiang River Basin. Nat Hazards 90:735–755. https://doi.org/10.1007/s11069-017-3068-z

MacLean A (2005) Statistical evaluation of WATFLOOD (Ms). University of Waterloo, Ontario

Mahmood R, Babel MS (2014) Future changes in extreme temperature events using the statistical downscaling model (SDSM) in the trans-boundary region of the Jhelum river basin. Weather Clim Extremes 5:56–66. https://doi.org/10.1016/j.wace.2014.09.001

Mesbahzadeh T, Miglietta MM, Mirakbari M, Soleimani Sardoo F, Abdolhoseini M (2019) Joint modeling of precipitation and temperature using copula theory for current and future prediction under climate change scenarios in arid lands (Case Study, Kerman Province, Iran). Adv Meteorol. https://doi.org/10.1155/2019/6848049

Micovic Z, Schaefer MG, Taylor GH (2015) Uncertainty analysis for probable maximum precipitation estimates. J Hydrol 521:360–337. https://doi.org/10.1016/j.jhydrol.2014.12.033

Moss RH, Edmonds JA, Hibbard KA, Manning MR, Rose SK, Van Vuuren DP, Carter TR, Emori S, Kainuma M, Kram T, Meehl GA, Mitchell JF, Nalicenovic N, Riahi K, Smith SJ, Stouffer RJ, Thomson AM, Weyant JP, Wilbanks TJ (2010) The next generation of scenarios for climate change research and assessment. Nature 463:747–756. https://doi.org/10.1038/nature08823

Nash JE, Sutcliffe JV (1970) River flow forecasting through conceptual models, part I: a discussion of principles. J Hydrol 10(3):282–290

Naseri Moghaddam M, Ghazanfari S, Ghahraman B, Davari K (2009) Probable maximum precipitation for 24-hour duration over four central provinces in Iran. In: World environmental and water resources congress, pp 1–6

Nobilis F, Haiden T, Kerschbaum M (1991) Statistical considerations concerning probable maximum precipitation (PMP) in the Alpine Country of Austria. Theor Appl Climatol 44:89–94. https://doi.org/10.1007/BF00867996

Palatella L, Miglietta MM, Paradisi P, Lionello P (2010) Climate change assessment for Mediterranean agricultural areas by statistical downscaling. Nat Hazards Earth Syst Sci 10:1647–1661

Papalexiou SM, Koutsoyiannis D (2006) A probabilistic approach to the concept of probable maximum precipitation. Adv Geosci 7:51–54

Raghunath HM (2006) Hydrology: principles, analysis and design. New Age International

Rahimi J, Ebrahimpour M, Khalili A (2013) Spatial changes of extended De Martonne climatic zones affected by climate change in Iran. Theor Appl Climatol 112(3–4):409–418. https://doi.org/10.1007/s00704-012-0741-8

Rakhecha PR, Singh VP (2009) Applied hydrometeorology. Springer, Berlin

Rakhecha PR, Mandal BN, Kulkarni AK, Deshpande NR (1995) Estimation of probable maximum precipitation for catchments in Eastern India by a generalized method. Theor Appl Climatol 51:67–74

Ramak Z, Porhemmat J, Sedghi H, Fattahi E, Lashni-Zand M (2017) The climate change effect on probable maximum precipitation in a catchment. A case study of the Karun river catchment in the Shalu bridge site (Iran). Russ Meteorol Hydrol 42(3):204–211. https://doi.org/10.3103/S1068373917030086

Rezacova D, Pesice P, Sokol Z (2005) An estimation of probable maximum precipitation for river basins in Czech Republic. J Atmos Res 77:407–421. https://doi.org/10.1016/j.atmosres.2004.10.011

Rouhani H, Leconte R (2016) A novel method to estimate the maximization ratio of the Probable Maximum Precipitation (PMP) using regional climate model output. Water Resour Res 52:7347–7365. https://doi.org/10.1002/2016WR018603

Salehnia N, Farid A, Hosseini F, Kolsoumi S, Zarrin A, Hasheminia M (2019) Comparing the performance of dynamical and statistical downscaling on historical run precipitation data over the semi-arid region. Asia-Pac J Atmospheric Sci 55(4):737–749. https://doi.org/10.1007/s13143-019-00112-1

Sehgal V, Lakhanpal A, Maheswaran R, Khosa R, Sridhar V (2018) Application of multi-scale wavelet entropy and multi-resolution Volterra models for climatic downscaling. J Hydrol 55:1078–1095. https://doi.org/10.1016/j.jhydrol.2016.10.048

Shaffie S, Mozaffari G, Khosravi Y (2019) Determination of extreme precipitation threshold and analysis of its effective patterns (case study: west of Iran). Nat Hazards 99:857–878. https://doi.org/10.1007/s11069-019-03779-x

Sharifi F, Samadi SZ, Wilson C (2012) Causes and consequences of recent floods in the Golestan catchments and Caspian Sea regions of Iran. Nat Hazards 61:533–550. https://doi.org/10.1007/s11069-011-9934-1

Shirdeli A (2012) Probable maximum precipitation 24 hours estimation, a case study of Zanjan province of Iran. Manag Sci Lett 2:2237–2242

Soltani M, Khoshakhlagh F, Zawar-Reza P, Miller STK, Molanejad M, Ranjbar Saadat Abadi A (2014) Probable maximum precipitation estimation using statistical and physical approaches over Esfahan province of Iran. Res J For Environ Prot 1:38–55

Trzaska S, Schnarr E (2014) A review of downscaling methods for climate change projections. United States Agency for International Development by Tetra Tech ARD, pp 1–42

Van Vuuren DP, Edmonds J, Kainuma M, Riahi K, Thomson A, Hibbard K, Hurtt GC, Kram T, Krey V, Lamarque JF, Masui T (2011) The representative concentration pathways: an overview. Clim Change 109:5–31. https://doi.org/10.1007/s10584-011-0148-z

Vivekanandan N (2015) Estimation of probable maximum precipitation using statistical methods. World J Res Rev (WJRR) 1:13–16

Wilby RL, Dawson CW (2004) SDSM 4.2: a decision support tool for the assessment of regional climate change impacts. User Guide

Wilby RL, Dawson CW (2007) SDSM 42: a decision support tool for the assessment of regional climate change impacts User manual

Wilby RL, Dawson CW, Barrow EM (2002) SDSM: a decision support tool for the assessment of regional climate change impacts. Environ Model Softw 17(2):145–157. https://doi.org/10.1016/S1364-8152(01)00060-3

World Meteorological Organization (WMO) (1986) Manual for estimation of probable maximum precipitation, operational hydrology report 1, 2nd edition, Publication 332. World Meteorological Organization, Geneva

World Meteorological Organization (1988) Analyzing long time series of hydrological data with respect to climate variability. World Meteorological Organization

World Meteorological Organization (WMO) (2009) Manual on estimation of probable maximum precipitation, 3rd edition, publication 1045, Geneva

Authors and Affiliations

Zahra Afzali-Gorouh[1] · Alireza Faridhosseini[1] · Bahram Bakhtiari[2] · Abolfazl Mosaedi[1] · Nasrin Salehnia[3,4]

Zahra Afzali-Gorouh
zahraafzali91@yahoo.com

Bahram Bakhtiari
drbakhtiari@uk.ac.ir

Abolfazl Mosaedi
mosaedi@um.ac.ir

Nasrin Salehnia
salehnia61@gmail.com

[1] Water Engineering Department, College of Agriculture, Ferdowsi University of Mashhad, Mashhad, Iran

[2] Water Engineering Department, Faculty of Agriculture, Shahid Bahonar University of Kerman, Kerman, Iran

[3] School of Earth and Environmental Sciences, Seoul National University, Seoul, South Korea

[4] Center for Cryospheric Sciences, Seoul National University, Siheung, South Korea